

ANALYSING THE STRUCTURAL, ELECTRONIC AND OPTICAL PROPERTIES OF Ca_3PbCl_3 PEROVSKITE FOR ITS APPLICABILITY IN GREEN ENERGY AND OPTOELECTRONIC APPLICATIONS

Chakshu Malan¹,  Krishna Kumar Mishra^{1*},  Rajnish Sharma²

¹Chitkara University Institute of Engineering and Technology, Chitkara University, Rajpura, Punjab-140401, India

²School of Engineering and Technology Chitkara University, Solan, Himachal Pradesh- 174103, India

*Corresponding Author e-mail: krishna.mishra@chitkara.edu.in

Received August 18, 2025; accepted October 6, 2025

The objective of this research is to provide a detailed examination of ways to improve the efficiency of perovskite Ca_3PbCl_3 in optoelectronic and solar cell applications. The substance known as Ca_3PbCl_3 is classified in the same category as perovskites that are composed of inorganic metal halides. In the scope of this study, the density functional theory (DFT), that are the base principle, was used to examine the optical, electrical, and structural characteristics. The generalized gradient approximation (GGA), the Perdew Burke–Ernzerhof functionals, and the linear combination of atomic orbital calculator are the tools that are utilized to gain an understanding of the characteristics of the Ca_3PbCl_3 perovskite. The key point includes the material's direct band gap, which is measured to be 20.35eV at the Γ -point. It has also been found that the dielectric function and absorption spectra change depending on the photon's energy. It has been reported that the extinction coefficient is 3.6963×10^4 and the refractive index is 1.4410. Therefore, studying Ca_3PbCl_3 's optical properties is crucial for considering this material for future use in photovoltaic and optoelectronic devices.

Keywords: Structural properties; Optical properties; Electrical properties; Layer separation

PACS: 71.20.-b, 77.22.-d, 78.20.Ci

1. INTRODUCTION

The significance of solar energy as a green, sustainable as well as enduring primary energy source is unquestionable. In comparison to conventional energy sources, solar photovoltaic technology clearly emerges as the superior choice. Photovoltaic cells efficiently convert light energy into electrical energy with minimal losses. Because of its widespread availability of irradiance absorption and allowable band gap for semiconductor devices, industrial photovoltaic systems are of major type. Additionally, their manufacturing process is very cost-effective. Perovskite compounds have garnered a lot of attention throughout the past few years as potential substitutions for traditional photovoltaic solar materials from a variety of fields. Silicon (Si), cerium titanate (CdTe), gallium arsenide (GaAs), and copper indium gallate selenide (CIGS) are all examples of such materials [1-4]. Having the capacity to absorb light across a wide range of wavelengths is absolutely necessary in order to create semiconductor devices that have the appropriate energy gap [5-7]. The operational characteristics of inorganic metal halide perovskites, Considerable attention has been created by their semiconducting solid-state nature, high absorption coefficients, and low reflection rates. [8-10].

During the last thirteen years, there has been a significant increase in the power conversion efficiency (PCE), which has risen from 3.8% to 26.1% [11-13]. Nevertheless, the extensive utilization of these potential attributes is made difficult by a lack of consistency. The perovskites' stability is extremely susceptible to moisture, air, light and temperature, making them particularly sensitive in real-world situations [14]. In the year 1839, Gustav Rose made the discovery of perovskite substance, which was subsequently called after the notable Russian mineralogist Lev Perovski. The term "perovskites" does not refer to the complex oxides of calcium and titanium (CaTiO_3) in particular rather, it refers to a group of chemicals that have the chemical formula ABX_3 , where X represents an anion whereas A and B represent cations of varying sizes, typically, A is cation of a bigger metal as compared to B [15-21]. Ions of transition metals usually occupy the B-site, while ions of rare earth or alkaline earth elements usually occupy the A-site. Particularly perovskite oxides are referred to by the symbol ABX_3 [22-24]. Furthermore, the development of solar cell technology has been greatly aided by ABX_3 cubic perovskites, which are characterized by high symmetry space group Pm-3m. The reason for this is that parity facilitates transitions in close proximity to the band edge, hence enhancing their light absorption capabilities and increasing their charge mobility. By adjusting the bandgaps of these materials, it becomes possible to have more versatility in capturing solar energy across a wider range of wavelengths, hence enhancing the structural advantages. Whereas Ca_3PbCl_3 , which is a perovskite compound, is advantageous in a number of ways, this material is well-suited for many technical uses, especially in the fields of photovoltaics and optoelectronics. Because it is suitable for large-scale manufacturing utilizing scalable fabrication techniques, Ca_3PbCl_3 demonstrates a tremendous potential for the creation of solar cells and optoelectronic devices that are both high-performance and cost-effective. Optoelectronic devices facilitate the development of connections between the structure, mechanism, characteristics, and performance of materials. These electrical devices are available in a wide variety of combinations. Efforts are currently underway to develop computational techniques that can improve the discovery of materials suitable for high-performance optoelectronic devices [25-30]. Furthermore, apart from the ongoing investigation

into innovative perovskite halide materials for possible application in solar cells and other optoelectronic devices, these materials can also be modified to possess flexibility and lightness, which provides a major benefit [31-35].

The selection of materials that are used in the production of flexible electronic devices has a significant impact on the performance, durability and flexibility of these devices within the industry. Combining a number of different materials makes it possible to create a technical gadget that may be used in a variety of contexts. As a result of its unique nature, which demonstrates great performance and technological priority, the halide perovskite is defined by its high level of cost-effectiveness and efficiency [36-42].

The aim is to address the discovered significant research gaps by concentrating on the different qualities. Possible results of this study include expanding our knowledge of perovskite material behaviour and encouraging the creation of new compositions that provide an environmentally friendly and practical substitute for current solar power systems, both of which aim to overcome the current limitations of perovskite solar cells.

Our methodological approach included calculating the density of states and band structure (DOS), and we have computed the elastic constants as well. The compound's stability was determined by using the Born-Huang inequality equations. Additionally, the mechanical constants, such as Young's modulus, shear modulus, and bulk modulus, were computed by employing the equations that relate to each of these constants. These equations offer extremely helpful information regarding the elasticity of the material as well as its capacity to withstand deformations.

Throughout the entirety of the work, there are four separate sections that have been incorporated. Within the introduction part, there is a description of the objectives and scope of our research. Presented in the second section is an explanation that is both clear and simple to understand of the computational methods that were applied. In the third section, our findings are reported and analyzed in detail. Each of the significant results and the consequences of those findings are detailed out in great detail in the fourth section. Based on the findings of the investigation, it offers a complete analysis and draws conclusions.

2. COMPUTATIONAL DETAILS

The primary objective of this research is to enhance the quality of Ca_3PCL_3 material that is used in the production of new perovskites. During the process of improving the bandgap, we explored its possible applications in the conversion of solar energy and in optoelectronic devices. In order to carry out the analysis, we use Quantum ATK software program to do computations based on the Density Functional Theory (DFT). Using the Materials Project database, we first gathered information about the A_3BX_3 type crystal, which contains 7 atoms per unit cell.

For the purpose of determining the structural properties of the novel perovskite Ca_3PCL_3 , calculations were carried out with the assistance of the exchange–correlation generalized gradient approximation (GGA) and the Perdew–Burke–Ernzerhof (PBE) functionals for linear combination of atomic orbitals (LCAO) calculator [43-45]. Quantum ATK Tool, version- 2023.12 was utilized in order to carry out these calculations.

The band structure and partial density of states of Ca_3PCL_3 both are analysed in Brillouin zone using computational methods. In order to get accurate computations, the Brillouin zone was partitioned into a grid of points using a K mesh of order $(5 \times 5 \times 5)$, with a density mesh cutoff of 60 Hartree. A convergence tolerance of 0.0001 was consistently maintained throughout the whole procedure. The process of optimization was modified by employing the Fermi–Dirac occupation approach over 9 self-consistent field phases. Both the Fast Fourier Transform (FFT) method and the Poisson solver have been applied. For the identification of eigen values, a medium pseudopotential was used. For calcium, PseudoDozo [$z=10$], PseudoDozo [$z=5$] for phosphorous and for chlorine it is PseudoDozo [$z=7$]. By this technique, researchers are able to get a deeper understanding of the material's potential that uses in a variety of fields, including semiconductor devices and catalysis, among others.

3 RESULTS AND DISCUSSION

3.1 Structural Properties:

Perovskites are a group of materials characterised by their distinctive crystal structure, which can be expressed by the formula ABX_3 . Ca_3PCL_3 belongs to the same chemical family with a Pm-3m cubic face and is formed of 7 atoms as its basic building block. Figure 1(a) displays the crystallographic structure of Ca_3PCL_3 , which forms in the Pm-3m space group, is indicated schematically.

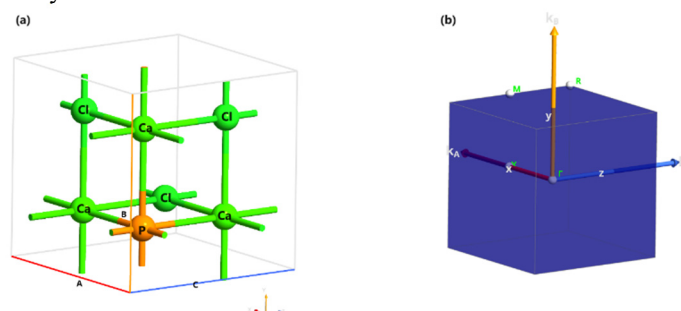


Figure 1. (a) The ideal framework of Ca_3PCL_3 perovskite and (b) k-path of Brillouin zone

Within the unit cell, the Cl atom is positioned at the edge of the face, The phosphorus atom is precisely located at the centre of the crystal, and the Ca atom is located at the vertex of the crystal. The k-path that is represented within the Brillouin zone (BZ) of the atomic structure is shown in Figure 1(b). Due to the high symmetry points (Γ -X-M- Γ -R-X-R-M), the Brillouin Zone occupies a position of great significance. The bond length of Ca-P and Ca-Cl in Ca_3PCl_3 perovskite material is 3.0005 Å. The behaviour of electrons at high-symmetry k-points is an important bit of information that is needed in order to have a thorough understanding of the conductivity, energy bandgap and electrical properties of the material.

To determine the minimum energy of the ground state and maintain the stability of the lattice, the lattice constant that leads to the lowest energy in the actual environment is of most significance. Lattice constant of Ca_3PCl_3 perovskite is 6.001Å as shown in Table 1. The rise in ion radius has been found to have a direct association with the modification of lattice constant, unit cell volume and density that has been discovered. Our optimization of the geometry turned out to be reliable with the comparison that had previously studied. The findings of our investigation indicated that the conclusions were in agreement with the findings of further theoretical studies that had been conducted. According to Apurba et.al [46] and Rasidul et.al [47], in their research they find the value of approximate to 6.00 Å as the lattice constant of Ca_3PCl_3 . With the help of the comparison, we were able to show that the approaches that we use to optimize geometry are accurate.

Table 1. Positioning of Ca_3PCl_3 lattice parameters

Material		Lattice constant (Å)	Lattice type	Unit cell volume	Space Group	Density
Ca_3PCl_3	Present study	6.001	Simple cubic	216.1Å ³	Pm-3m (221)	1.979 g/cm ³
	Others study	5.69 [46]	Simple cubic	-	Pm-3m (221)	-
		5.725 [47]	Simple cubic	-	Pm-3m (221)	-

In addition, by analysing their mechanical characteristics by examining the elastic properties of system. Fundamental elastic constants that are C_{11} , C_{22} and C_{44} , can be used to evaluate the mechanical properties of perovskite [48-49]. According to the findings of our research, the values of C_{11} , C_{12} , and C_{44} are 44.78, 11.25 and 15.82 respectively as shown in Table 2. The Born-Huang stability criteria have become known as the necessary conditions for a cubic structure to be stable, $C_{44} > 0$, $C_{11} - C_{12} > 0$ and $C_{11} + 2C_{12} > 0$. Furthermore, the elastic constants were used to establish the material properties, such as the Bulk modulus, shear modulus and Young's modulus, in order to determining the ductility and brittleness of a material [50-53]. On the other hand, poissons ratio that is calculated is 0.2008 which measures the number of dimensional changes that occur when a material is subjected to a load. Mechanical properties make this material perfect for flexible electronics. Solar cells and data storage systems that need regular performance satisfying the needs of modern applications that require strength and flexibility.

Table 2. The calculated values of elastic constants of the Ca_3PCl_3 compound

Material	C_{11}	C_{12}	C_{44}	Bulk modulus (B)	Shear modulus (G)	Young's modulus (Y)
Ca_3PCl_3	44.78	11.25	15.82	22.4245	16.2002	40.2578

2.2 Electronics Properties

3.2.1 Band Structure

A substance's electronic properties are those that pertain to creation and flow of electrons inside its molecular structure [54]. Understanding the electronic band structure allows one to predict the electron behaviour in materials, light absorption and electrical conductivity. The band structure and the electron density of states are the two types of properties that are associated with electrical devices [55].

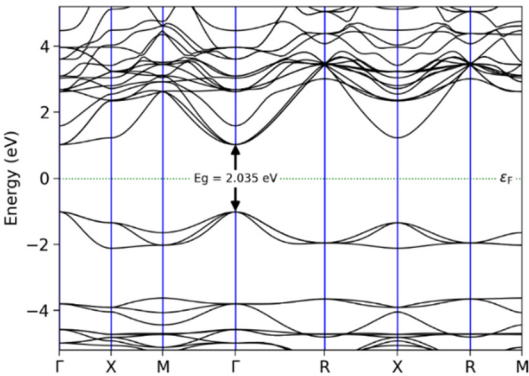


Figure 2. The electronic band structures of Ca_3PCL_3 perovskite

A representation of the energy band structure of Ca_3PCL_3 with BZ points (Γ -X-M- Γ -R-X-R-M) is presented in Fig. 2, encompassing a range of -5 to 5 electron volts. In Table 3, Ca_3PCL_3 has been shown to have a direct band gap of 2.035 eV,

while the CBE is 1.0189 eV and the VBE is -1.0163 eV from measurements that were taken. It is at the Γ -point, which is the central point within the Brillouin zone, that the conduction band and the valence band exhibit their lowest and highest energy points, respectively. This characteristic is preferable for optoelectronic devices, as it indicates the potential for effective charge carrier mobility.

Materials with a bandgap lower than 3.1 electron volts hold great potential for the development of devices that utilize visible light. Across the energy range of 1.2-12.3 eV, the perovskite exhibits considerable differences in its optical features, which makes it suitable for use, such as light-emitting diodes (LEDs) or photodetectors that are designed to detect ultraviolet light, as well as solar cells that are purpose-built to detect visible light [56]. Based on the calculations, Ca_3PCL_3 has a direct band gap, making it a perfect material for use in optoelectronic devices.

Table 3. Electrical Properties of Ca_3PCL_3 Perovskite

Material	Direct Bandgap (eV)		CBE (eV)	VBE (eV)	Layer separation (\AA)
Ca_3PCL_3	Present study	2.035	1.0189	-1.0163	6.00
	Pervious study	2.208[46]	-	-	-
		2.109[47]	-	-	-

3.2.2 Complex Band Structure

A material's transport characteristics can be derived from its complex band structure, which also allows in identifying the charge carriers that contribute to tunnelling currents within the band gap. There are two different sorts of modes that are included in the complex band structure (CB), these modes are a propagating mode and a decaying mode, as shown in Fig. 3. It is possible to make use of the value of the wave vector (k) that has been provided for any of the two different sorts of modes. Within the same directional spectrum, decaying modes are described by a complex Bloch phase factor, whereas propagating modes are characterized by a real Bloch phase factor in the direction opposite to the C axis.

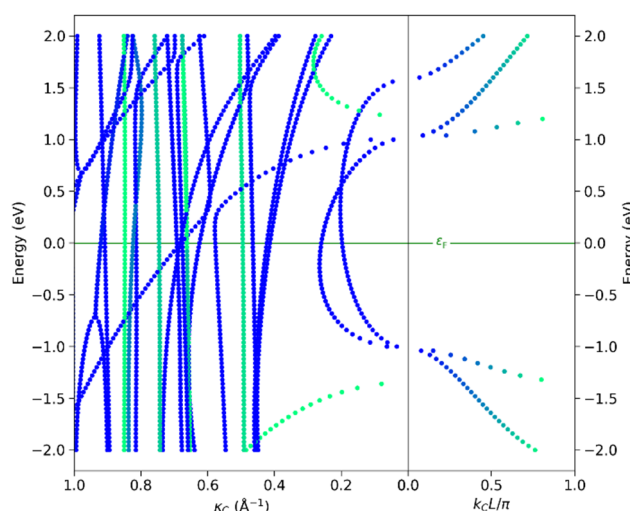


Figure 3. Complex band structure of novel perovskite Ca_3PCL_3

In the field of optoelectronics, our investigation of the CBS aims to throw provide light on the potential applications of these materials. The real values of k_c represent the conventional Bloch states, which are observed on the right side of the diagram. Conversely, complex k_c values are associated with states that are in proximity to the material's surface. With a layer separation of 6.00 \AA , the presence of Ca_3PCL_3 is shown by the CBS. Therefore, this study's findings show that the novel Ca_3PCL_3 perovskite halide is a great material to employ in the production of optoelectronic devices.

3.2.3 Density of State

When it comes to the perovskite halide Ca_3PCL_3 , the density of states (DOS) is all about how the electronic states are ordered throughout the material's different energy levels. This is related to the composition of the substance. By utilising density of states, one can find out considerable amount of information about the electrical structure and characteristics of the materials. Crystal structure, bandgap and electron density between atoms are three important variables that define the DOS.

Fig. 4 shows the distribution of density of states for Ca_3PCL_3 . It covers an energy range from -5 to 5 eV. The energy spectrum is fully occupied by the hybrid states of phosphorous (P) and calcium (Ca) in conjunction with chlorine (Cl). Density of states identifies peaks at -4.7 eV, -3.8 eV and -1.9 eV within the valence band (left side) and 4.4 eV, 3.4 eV and 3.3eV in the conduction band (right side). In optoelectronic applications, direct bandgap semiconductors are frequently chosen because of their exceptional efficiency in optoelectronic conversions and solar cells, this paper details the electrical properties of Ca_3PCL_3 , offering insight into its potential usage.

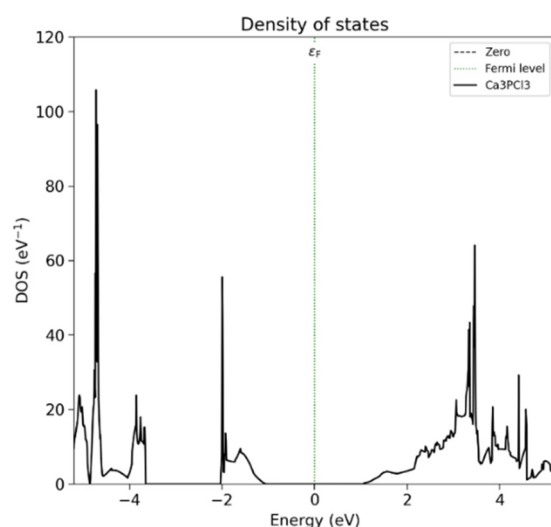


Figure 4. Total density of states of novel perovskite Ca_3PbCl_3

3.2.4 Projected Density of States

Projected density of states (PDOS) of Ca_3PbCl_3 provides information about the distribution of electronic states among the calcium, phosphorus and chlorine atoms. It gives information regarding the electrical configuration of the compound as well as the bonding characteristics that are important when knowing its properties in various applications. This illustrates the way in which orbitals from each individual atom contribute to the overall density of states of the complex [57-58].

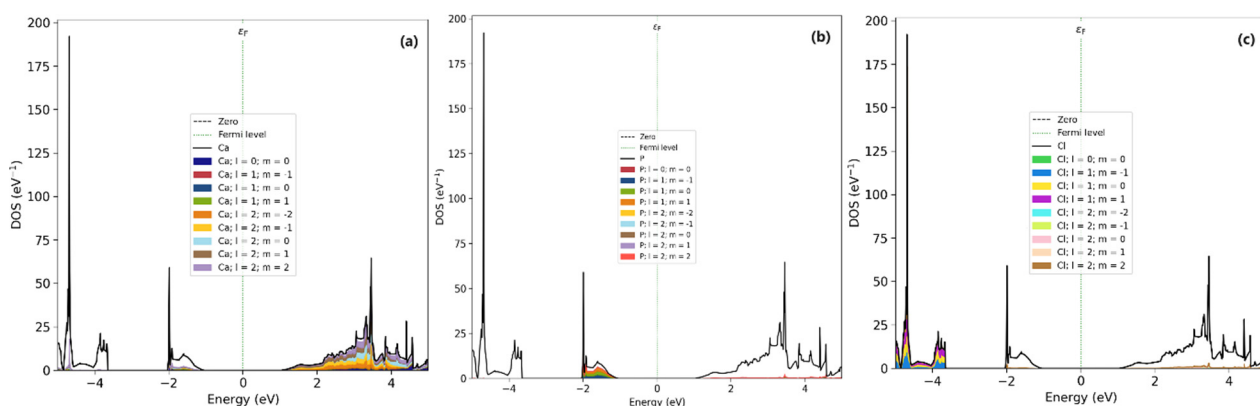


Figure 5. Projected density of states of Ca_3PbCl_3 perovskite

The calculation of a PDOS takes place using an energy range from (-5 to 5 eV). Figure 5 (a-c) shows the PDOS of particular atoms of Ca_3PbCl_3 . According to the results of our research, the p-orbital densities of phosphorus (P) and chlorine (Cl) have a significant impact on the behaviour of the valence band (VB) also the calcium d-orbital has an effect on the conduction band (CB). The presence of these energy levels allows for a diverse variety of electron states to make contributions to the valence band.

3.2.5 Electron Density

The electron density distribution forms a cloud around the atoms during the bonding process. As the density of this cloud increases, it represents the probability of an electron being found in a certain location. For stronger bonding interactions, a higher density is preferred. When attempting to identify the electronic properties of a material, it is necessary to investigate the electronic charge density of the material [59-61]. Presented in Figure 6(a) is a two-dimensional representation of the crystallographic plane. Each colour on the bottom-right scale bar represents a different strength of the electron density.

An illustration of a viewpoint that appears to be comparable to that of a bird's eye view may be obtained from Figure 6(b). It is much simpler to understand the manner in which the charges are dispersed surrounding the atoms in different amounts within the structure. The three dimension image of charge distribution can be seen in Fig. 6(c), from this one can acquire a comprehensive understanding of the distributing of charges around atoms with different levels of intensity.

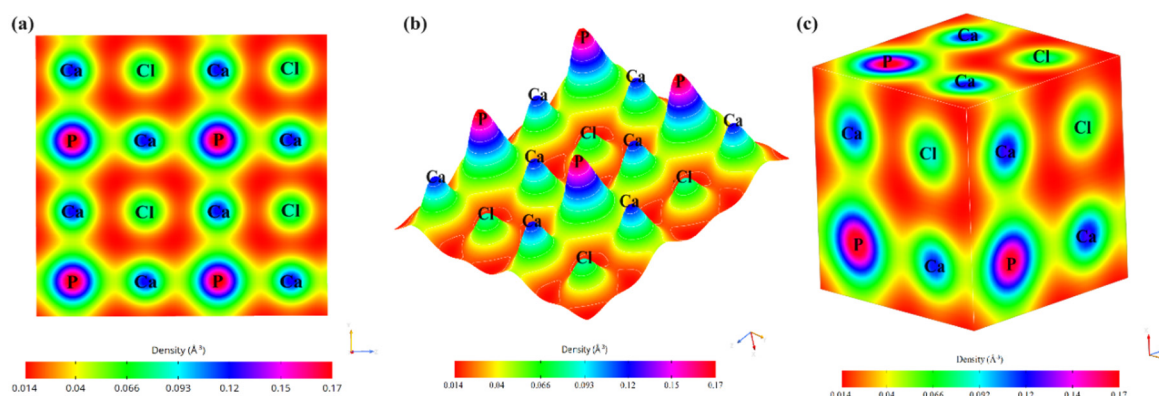


Figure 6. The charge density distribution of Ca_3PCL_3 can be visually represented in three different ways: (a) a two-dimensional depiction, (b) a top-down perspective resembling a bird's eye view, and (c) a three-dimensional view

3.3 Optical Properties

These properties of Ca_3PCL_3 make it highly suitable for extensive application in the field of optoelectronics. Thorough testing is necessary to ascertain the suitability of materials for application in solar cell and optoelectronic devices [62]. Several optical properties, including as the absorption coefficient, conductivity, dielectric functions, reflectivity, extension coefficient and refractive index, are included in the of this study and shown in Table 4. A material's optical qualities are affected by its light-reactivity and light-adjustment capabilities, which are in turn affected by its interaction with light. In the following equation of the dielectric function, the real and imaginary parts are denoted by the symbols ($\text{Re}(\epsilon)$) as well as ($\text{Im}(\epsilon)$), respectively.

$$\epsilon = \text{Re}(\epsilon) + \text{Im}(\epsilon) \quad (1)$$

Where absorption coefficient indicates that it has improved capacity to absorb light of varying wavelengths as compared to other compounds. The real and imaginary dielectric functions can be used to calculate absorption coefficient. The absorption coefficient of a perovskite made of Ca_3PCL_3 has been shown in Figure 7(a).

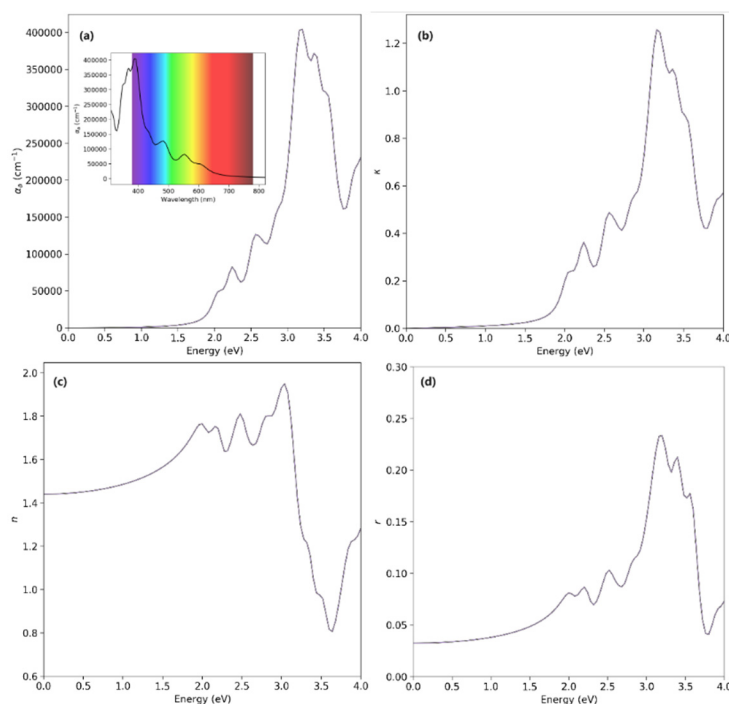


Figure 7. The real coefficients of optical constants Ca_3PCL_3 : (a) absorption coefficient (α), (b) extinction coefficient (κ), (c) refractive index (n) and (d) reflectivity (r)

From the observed value, the highest absorption peak is observed at 3.2 eV, corresponding to 404615 cm^{-1} . This, in turn, would raise the competitiveness of these materials in the market for solar components. Whereas, the extinction coefficient is a measure of the reduction in electromagnetic radiation within a substance, determined by measuring the imaginary part of the refractive index. On the other hand, the real component denotes the velocity at which EM waves travel through the substance. The material Ca_3PCL_3 exhibits a low κ value of 0 eV, suggesting its minimum absorption at low energies (3.6963×10^{-5}) as shown in Fig. 7(b). The refractive index (n) is a quantitative measure used to determine the

stability of a material in different device applications by measuring the changes in the speed of light within the material. This specific parameter is an aspect of the complex interaction that occurs between light and a material. In Fig 7(c), the material's refractive index, indicating a substantial level of light interaction within this energy range during its propagation. When developing antireflective layers for solar cells, it is feasible to utilize materials with a high refractive index [63]. The calculated value of refractive index is 1.4410. Furthermore, when subjected to electromagnetic radiation, including visible light, Ca_3PCL_3 perovskite exhibits a certain quantity of light that it reflects. Depending on a variety of parameters, including surface shape, crystal orientation and composition, perovskite materials can display significant changes in their overall reflectance [64]. However, the reflectivity of the Ca_3PCL_3 perovskite can be affected by both the wavelength of light and the angle of contact with the substance. The reflectivity of Ca_3PCL_3 is 0.0326, as depicted in Fig 7(d).

Ca_3PCL_3 complex coefficient reflects the compound's geometric image's imaginary unit coefficient. The chemical composition Ca_3PCL_3 contains calcium, phosphorus, and chlorine. Under certain conditions, a molecule with an imaginary coefficient may undergo complex bonding or phase transition.

Table 4. Real and optical properties of Ca_3PCL_3 perovskite

Material	Properties		Units	Values
Ca_3PCL_3	Real	Absorption coefficient	cm^{-1}	404615 (3.2 eV)
		Extinction coefficient	-	3.6963×10^{-5}
		Refractive Index	-	1.4410
		Reflectivity	-	0.0326
	Complex	Optical Conductivity	$\text{AV}^{-1}\text{cm}^{-1}$	1760.05 (3.12 eV)
		Dielectric constant	-	2.0766
		Polarizability	cm^2v^{-1}	2.0602×10^{-39}
		Susceptibility	-	1.0766

Optical conductivity is a property of a material that quantifies the correlation between the magnitude of the electric current generated in the material and its current density, leading to the generation of an electric field at a particular frequency [65]. As shown in Fig. 8(a) the value of real optical conductivity is $1760.05 \text{ AV}^{-1}\text{cm}^{-1}$ at 3.12 eV. Whereas the real part of the dielectric constants predicts the value of 2.0766, as shown in Fig 8(b), indicating reduced internal power dissipation.

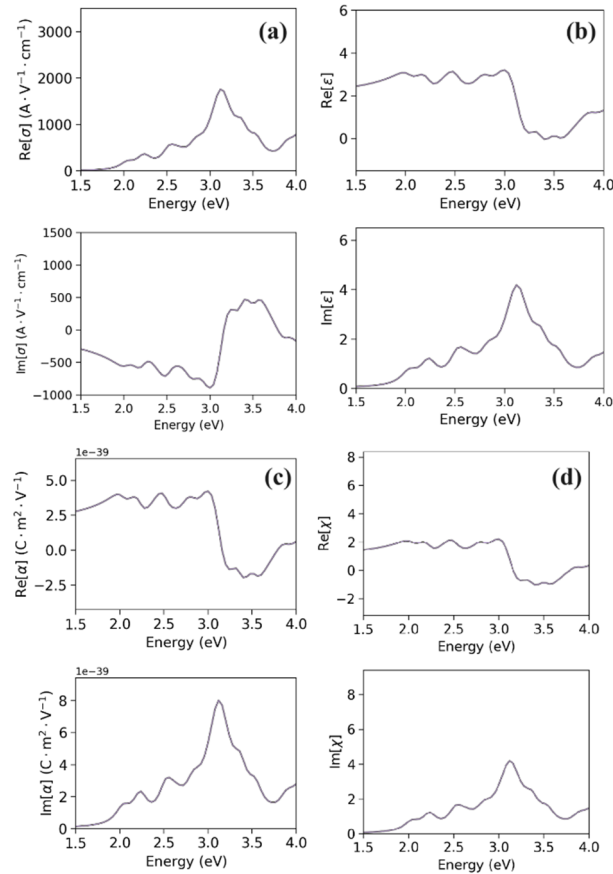


Figure 8. The optical constants Ca_3PCL_3 are determined by the complex coefficients of optical conductivity (σ), dielectric constant (ϵ), polarizability (α), and susceptibility (χ)

This is beneficial for enhancing solar cell efficiency. Furthermore, the actual $\text{Re}[\alpha]$ component of dielectric constant represents influence of polarization and dispersion on material. Figure 8 (c) depicts the polarizability of recently discovered halide perovskite. This graphic includes both the real $\text{Re}[\alpha]$ polarizability and an imaginary $\text{Im}[\alpha]$ polarizability. The real polarizability value of Ca_3PbCl_3 is $2.0602 \times 10^{-39} \text{ cm}^2 \text{ V}^{-1}$. We have also calculated the value of susceptibility of Ca_3PbCl_3 as shown in Fig 8(d), the calculated real value $\text{Re}[\chi]$ is 1.0766 reported in our work. According to the findings, Ca_3PbCl_3 possesses excellent features for converting solar energy, especially in terms of its optical conductivity, which makes it best use in solar cells.

CONCLUSIONS

In a nutshell, our investigation consisted of utilizing DFT calculation in order to investigate the material Ca_3PbCl_3 , with a particular emphasis on the structures, optical properties, electrical properties, and mechanical properties of the material. The value of 2.035 eV was discovered to represent the direct bandgap of Ca_3PbCl_3 . The material Ca_3PbCl_3 exhibits exceptional potential for application in the fields of solar cells and optoelectronics. Additionally, the computed elastic constants for this structure were as follows: $C_{11} = 744.78$, $C_{12} = 11.25$ and $C_{44} = 15.82$. Whereas the calculated value of refractive index is 1.4410. This is because it offers crucial information regarding the propagation of light through a substance. As it explains the phenomenon of light propagation through a material. However, the value of dielectric constant is 2.0766 also the calculated value of extinction coefficient is 3.69638×10^5 , which can be used to calculate the ability of a molecule to absorb light at a particular frequency. The findings of this work are expected to provide guidance for the development of flexible electronic devices, such as solar cells, optoelectronic devices, and other devices that could potentially make use of this material due to its potential applications.

ORCID

©Krishna Kumar Mishra, <https://orcid.org/0000-0001-6888-7654>; ©Rajnish Sharma, <https://orcid.org/0000-0001-8644-016X>

REFERENCES

- [1] M. Victoria, N. Haegel, I.M. Peters, R. Sinton, A. Jäger-Waldau, C. del Canizo, C. Breyer, et al. "Solar photovoltaics is ready to power a sustainable future," *Joule*, **5**(5), 1041-1056 (2021). <https://doi.org/10.1016/j.joule.2021.03.005>
- [2] T. Jackson, and M. Oliver, "The viability of solar photovoltaics," *Energy policy*, **28**(14), 983-988 (2000). [https://doi.org/10.1016/S0301-4215\(00\)00085-9](https://doi.org/10.1016/S0301-4215(00)00085-9)
- [3] Md.F. Rahman, J. Hossain, A. Kuddus, S. Tabassum, M.H.K. Rubel, Md.M. Rahman, Y. Moriya, et al. "A novel CdTe ink-assisted direct synthesis of CdTe thin films for the solution-processed CdTe solar cells," *Journal of materials science*, **55**, 7715-7730 (2020). <https://doi.org/10.1007/s10853-020-04578-7>
- [4] M.K. Hossain, G.F.I. Toki, D.P. Samajdar, M. Mushtaq, M.H.K. Rubel, R. Pandey, J. Madan, et al. "Deep insights into the coupled optoelectronic and photovoltaic analysis of lead-free CsSnI_3 perovskite-based solar cell using DFT calculations and SCAPS-1D simulations," *ACS omega*, **8**(25), 22466-22485 (2023). <https://doi.org/10.1021/acsomega.3c00306>
- [5] Q. Ma, S. Huang, S. Chen, M. Zhang, C.F.J. Lau, M.N. Lockrey, H.K. Mulmudi, et al. "The effect of stoichiometry on the stability of inorganic cesium lead mixed-halide perovskites solar cells," *The Journal of Physical Chemistry C*, **121**(36), 19642-19649 (2017). <https://doi.org/10.1021/acs.jpcc.7b06268>
- [6] Md.E. Islam, Md.R. Islam, S. Ahmmed, M.K. Hossain, and Md.F. Rahman, "Highly efficient SnS-based inverted planar heterojunction solar cell with ZnO ETL," *Physica Scripta*, **98**(6), 065501 (2023). <https://doi.org/10.1088/1402-4896/acb13>
- [7] Y. Zhou, L. You, S. Wang, Z. Ku, H. Fan, D. Schmidt, A. Rusydi, et al. "Giant photostriction in organic-inorganic lead halide perovskites," *Nature communications*, **7**(1), 11193 (2016). <https://doi.org/10.1038/ncomms11193>
- [8] M.M. Abdelhamied, Y. Song, W. Liu, X. Li, H. Long, K. Wang, B. Wang, and P. Lu, "Improved photoemission and stability of 2D organic-inorganic lead iodide perovskite films by polymer passivation," *Nanotechnology*, **31**(42), 42LT01 (2020). <https://doi.org/10.1088/1361-6528/aba140>
- [9] J. Di, J. Chang, and S. Liu, "Recent progress of two-dimensional lead halide perovskite single crystals: crystal growth, physical properties, and device applications," *EcoMat*, **2**(3), e12036 (2020). <https://doi.org/10.1002/eom2.12036>
- [10] S. Wu, Z. Li, M.-Q. Li, Y. Diao, F. Lin, T. Liu, J. Zhang, et al. "2D metal-organic framework for stable perovskite solar cells with minimized lead leakage," *Nature Nanotechnology*, **15**(11), 934-940 (2020). <https://doi.org/10.1038/s41565-020-0765-7>
- [11] W. Shen, Y. Zhao, and F. Liu, "Highlights of mainstream solar cell efficiencies in 2021," *Front. Energy*, **16**, 1-8 (2022). <https://doi.org/10.1007/s11708-022-0816-x>
- [12] H. Liu, L. Xiang, P. Gao, D. Wang, J. Yang, X. Chen, S. Li, Y. Shi, F. Gao, and Y. Zhang, "Improvement strategies for stability and efficiency of perovskite solar cells," *Nanomaterials*, **12**(19), 3295 (2022). <https://doi.org/10.3390/nano12193295>
- [13] P. Roy, N.K. Sinha, S. Tiwari, and A. Khare, "A review on perovskite solar cells: Evolution of architecture, fabrication techniques, commercialization issues and status," *Solar Energy*, **198**, 665-688 (2020). <https://doi.org/10.1016/j.solener.2020.01.080>
- [14] Y. Yuan, J. Chae, Y. Shao, Q. Wang, Z. Xiao, A. Centrone, and J. Huang, "Photovoltaic switching mechanism in lateral structure hybrid perovskite solar cells," *Advanced Energy Materials*, **5**(15), (2015). <https://doi.org/10.1002/aenm.201500615>
- [15] K. Zheng, and T. Pullerits, "Two dimensions are better for perovskites," *The Journal of Physical Chemistry Letters*, **10**(19), 5881-5885 (2019). <https://doi.org/10.1021/acs.jpcclett.9b01568>
- [16] G.E. Eperon, S.D. Stranks, C. Menelaou, M.B. Johnston, L.M. Herz, and H.J. Snaith, "Formamidinium lead trihalide: a broadly tunable perovskite for efficient planar heterojunction solar cells," *Energy & Environmental Science*, **7**(3), 982-988 (2014). <https://doi.org/10.1039/C3EE43822H>
- [17] Mishra, Krishna Kumar, "Exploring the physical, electrical and optical properties of $\text{Cs}_2\text{LiInBr}_6$ Perovskite: an extensive study utilizing DFT based GGA-PBE and HSE06 functionals." *Brazilian Journal of Physics*, **55**(1), 31 (2025). <https://doi.org/10.1007/s13538-024-01653-1>
- [18] B. Wang, J. Iocozzia, M. Zhang, M. Ye, S. Yan, H. Jin, S. Wang, Z. Zou, and Z. Lin, "The charge carrier dynamics, efficiency and stability of two-dimensional material-based perovskite solar cells," *Chemical Society Reviews*, **48**(18), 4854-4891 (2019). <https://doi.org/10.1039/c9cs00254e>

- [19] G.M. Wilson, M. Al-Jassim, W.K. Metzger, S.W. Glunz, P. Verlinden, G. Xiong, L.M. Mansfield, *et al.* “The 2020 photovoltaic technologies roadmap,” *Journal of Physics D: Applied Physics*, **53**(49), 493001 (2020). <https://doi.org/10.1088/1361-6463/ab9c6a>
- [20] M. Aaogi, Y. Shirako, H. Kojitani, T. Nagakari, H. Yusa, and K. Yamaura, “High-pressure transitions in NaZnF_3 and NaMnF_3 perovskites, and crystal-chemical characteristics of perovskite–postperovskite transitions in ABX_3 fluorides and oxides,” *Physics of the Earth and Planetary Interiors*, **228**, 160–169 (2014). <https://doi.org/10.1016/j.pepi.2013.09.001>
- [21] A. Alhashmi, M.B. Kanoun, and S. Goumri-Said, “Machine learning for halide perovskite materials ABX_3 (B= Pb, X= I, Br, Cl) assessment of structural properties and band gap engineering for solar energy,” *Materials*, **16**(7), 2657 (2023). <https://doi.org/10.3390/ma16072657>
- [22] R.S. Roth, “Classification of perovskite and other ABO_3 -type compounds,” *Journal of Research of the National Bureau of Standards*, **58**(2), 75–88 (1957). <https://doi.org/10.6028/jres.058.010>
- [23] C. Moure, and O. Peña, “Recent advances in perovskites: Processing and properties,” *Progress in Solid State Chemistry*, **43**(4), 123–148 (2015). <https://doi.org/10.1016/j.progsolidstchem.2015.09.001>
- [24] X. Liu, J. Fu, and G. Chen, “First-principles calculations of electronic structure and optical and elastic properties of the novel ABX_3 -type LaWN_3 perovskite structure,” *RSC advances*, **10**(29), 17317–17326 (2020). <https://doi.org/10.1039/c9ra10735e>
- [25] H.-J. Feng, and Q. Zhang, “Predicting efficiencies > 25% A_3MX_3 photovoltaic materials and Cu ion implantation modification,” *Applied Physics Letters*, **118**(11), (2021). <https://doi.org/10.1063/5.0039936>
- [26] Md.F. Rahman, Md. Al Ijajul Islam, Md.R. Islam, Md.H. Ali, P. Barman, Md.A. Rahman, Md. Harun-Or-Rashid, *et al.* “Investigation of a novel inorganic cubic perovskite Ca_3PI_3 with unique strain-driven optical, electronic, and mechanical properties,” *Nano Select*, (2023). <https://doi.org/10.1002/nano.202300066>
- [27] Y. Li, and K. Yang, “High-throughput computational design of halide perovskites and beyond for optoelectronics,” *Wiley Interdisciplinary Reviews: Computational Molecular Science*, **11**(3), e1500 (2021). <https://doi.org/10.1002/wcms.1500>
- [28] S. Binetti, M. Acciarri, A. Le Donne, M. Morgano, and Y. Jestin, “Key success factors and future perspective of silicon-based solar cells,” *International Journal of Photoenergy*, **2013**(1), 249502 (2013). <https://doi.org/10.1155/2013/249502>
- [29] J. Singh, and A. Agrahari, “The progression of silicon technology acting as substratum for the betterment of future photovoltaics,” *International Journal of Energy Research*, **43**(9), 3959–3980 (2019). <https://doi.org/10.1002/er.4402>
- [30] J. Shim, E.-K. Lee, Y.J. Lee, and R.M. Nieminen, “Density-functional calculations of defect formation energies using the supercell method: Brillouin-zone sampling,” *Physical Review B—Condensed Matter and Materials Physics*, **71**(24), 245204 (2005). <https://doi.org/10.1103/physrevb.71.245204>
- [31] S. Luo, T. Li, X. Wang, M. Faizan, and L. Zhang, “High-throughput computational materials screening and discovery of optoelectronic semiconductors,” *Wiley Interdisciplinary Reviews: Computational Molecular Science*, **11**(1), e1489 (2021). <https://doi.org/10.1002/wcms.1489>
- [32] Z. Liu, G. Na, F. Tian, L. Yu, J. Li, and L. Zhang, “Computational functionality-driven design of semiconductors for optoelectronic applications,” *InfoMat*, **2**(5), 879–904 (2020). <https://doi.org/10.1002/inf2.12099>
- [33] S. Kang, D. Lee, J. Kim, A. Capasso, H.S. Kang, J.-W. Park, C.-H. Lee, and G.-H. Lee, “2D semiconducting materials for electronic and optoelectronic applications: potential and challenge,” *2D Materials*, **7**(2), 022003 (2020). <https://doi.org/10.1088/2053-1583/ab6267>
- [34] Y. Xue, T. Yang, Y. Zheng, K. Wang, E. Wang, H. Wang, L. Zhu, *et al.* “Heterojunction engineering enhanced self-polarization of $\text{PVDF/CsPbBr}_3/\text{Ti}_3\text{C}_2\text{T}_x$ composite fiber for ultra-high voltage piezoelectric nanogenerator,” *Advanced Science*, **10**(18), 2300650 (2023). <https://doi.org/10.1002/adv.202300650>
- [35] M. Pagliaro, R. Ciriminna, and G. Palmisano, “Flexible solar cells,” *ChemSusChem: Chemistry & Sustainability Energy & Materials*, **1**(11), 880–891 (2008). <https://doi.org/10.1002/cssc.200800127>
- [36] K. Rana, J. Singh, and J.-H. Ahn, “A graphene-based transparent electrode for use in flexible optoelectronic devices,” *Journal of Materials Chemistry C*, **2**(15), 2646–2656 (2014). <https://doi.org/10.1039/c3tc32264e>
- [37] Y.-F. Liu, J. Feng, Y.-G. Bi, D. Yin, and H.-B. Sun, “Recent developments in flexible organic light-emitting devices,” *Advanced Materials Technologies*, **4**(1), 1800371 (2019). <https://doi.org/10.1002/admt.201800371>
- [38] J. Lewis, “Material challenge for flexible organic devices,” *Materials today*, **9**(4), 38–45 (2006). [https://doi.org/10.1016/S1369-7021\(06\)71446-8](https://doi.org/10.1016/S1369-7021(06)71446-8)
- [39] S. Chahar, P. Sharma, K.K. Mishra, and R. Sharma, “A Review Article on the usage of Different Materials and Different Device architectures in the Design of Tunnel Field Effect Transistor,” in: *2022 IEEE International Conference of Electron Devices Society Kolkata Chapter (EDKCON)*, (IEEE, 2022), pp. 592–597.
- [40] Y. Wang, S. Bai, L. Cheng, N. Wang, J. Wang, F. Gao, and W. Huang, “High-efficiency flexible solar cells based on organometal halide perovskites,” *Advanced Materials*, **28**(22), 4532–4540 (2016). <https://doi.org/10.1002/adma.201504260>
- [41] Q. Chen, N. De Marco, Y.M. Yang, T.-B. Song, C.-C. Chen, H. Zhao, Z. Hong, *et al.* “Under the spotlight: The organic–inorganic hybrid halide perovskite for optoelectronic applications,” *Nano Today*, **10**(3), 355–396 (2015). <https://doi.org/10.1016/j.nantod.2015.04.009>
- [42] S. Huang, Y. Liu, Y. Zhao, Z. Ren, and C.F. Guo, “Flexible electronics: stretchable electrodes and their future,” *Advanced Functional Materials*, **29**(6), 1805924 (2019). <https://doi.org/10.1002/adfm.201805924>
- [43] J.P. Perdew, J.A. Chevary, S.H. Vosko, K.A. Jackson, M.R. Pederson, D.J. Singh, and C. Fiolhais, “Atoms, molecules, solids, and surfaces: Applications of the generalized gradient approximation for exchange and correlation,” *Physical review B*, **46**(11), 6671 (1992). <https://doi.org/10.1103/physrevb.46.6671>
- [44] J.P. Perdew, K. Burke, and M. Ernzerhof, “Generalized gradient approximation made simple,” *Physical review letters*, **77**(18), 3865 (1996). <https://doi.org/10.1103/physrevlett.77.3865>
- [45] QuantumATK version U-2023.09, Synopsys QuantumATK, <https://www.synopsys.com/silicon/quantumatk.html> (accessed: October 2023).
- [46] I.K.G.G. Apurba, Md.R. Islam, Md.S. Rahman, Md.F. Rahman, and J. Park, “Tuning the physical properties of inorganic novel perovskite materials Ca_3PX_3 (X= I, Br and Cl): Density function theory,” *Heliyon*, **10**(7), (2024). <https://doi.org/10.1016/j.heliyon.2024.e29144>
- [47] Md.R. Islam, A. Zahid, M.A. Rahman, Md.F. Rahman, M.A. Islam, M.K. Hossain, M.A. Ali, M.A. Iqbal, F.I. Bakhsh, and S. Ahmad, “Tuning the optical, electronic, and mechanical properties of inorganic Ca_3PCl_3 perovskite via biaxial strain,” *Journal of Physics and Chemistry of Solids*, **184**, 111722 (2024). <https://doi.org/10.1016/j.jpcs.2023.111722>

- [48] S.-J. Zou, Y. Shen, F.-M. Xie, J.-D. Chen, Y.-Q. Li, and J.-X. Tang, "Recent advances in organic light-emitting diodes: toward smart lighting and displays," *Materials Chemistry Frontiers*, **4**(3), 788-820 (2020). <https://doi.org/10.1039/C9QM00716D>
- [49] Q. Dai, Q.-Q. Liang, T.-Y. Tang, H.-X. Gao, S.-Q. Wu, and Y.-L. Tang, "The structural, stability, electronic, optical and thermodynamic properties of Ba_2AsXO_6 (X= V, Nb, Ta) double perovskite oxides: A First-Principles study," *Inorganic Chemistry Communications*, **166**, 112591 (2024). <https://doi.org/10.1016/j.inoche.2024.112591>
- [50] T. Tang, and Y. Tang, "First principle comparative study of transitional elements Co, Rh, Ir (III)-based double halide perovskites," *Materials Today Communications*, **34**, 105431 (2023). <https://doi.org/10.1016/j.mtcomm.2023.105431>
- [51] T. Yao, Y. Wang, H. Li, J. Lian, J. Zhang, and H. Gou, "A universal trend of structural, mechanical and electronic properties in transition metal (M= V, Nb, and Ta) borides: First-principle calculations," *Computational materials science*, **65**, 302-308 (2012). <https://doi.org/10.1016/j.commatsci.2012.07.021>
- [52] Md.A. Rahman, I. Ria, A. Ghosh, A.A.A. Bahajaj, and R.J. Ramalingam, "A Novel Investigation into Strain-Induced Changes in the Physical Properties of Lead-Free Ca_3SnCl_3 Perovskite," Preprint, <https://dx.doi.org/10.2139/ssrn.4782983>
- [53] F. Mouhat, and F.-X. Coudert, "Necessary and sufficient elastic stability conditions in various crystal systems," *Physical review B*, **90**(22), 224104 (2014). <https://doi.org/10.1103/PhysRevB.90.224104>
- [54] M. Maghrabi, A.Y. Al-Reyahi, N. Al Aqtash, S.M. Al Azar, A. Shaheen, A. Mufleh, and B. Shaban, "Investigating the physical properties of lead-free halide double perovskites $\text{Cs}_2\text{AgXBr}_6$ (X= P, As, Sb) for photovoltaic and thermoelectric devices using the density functional theory," *Materials Today Communications*, **37**, 107541 (2023). <https://doi.org/10.1016/j.mtcomm.2023.107541>
- [55] K.K. Mishra, "Study on Structural, Mechanical, Electronic, Vibrational, Optical and Thermo-Dynamical Behaviour of ZB Structured BeZ (Z=S, Se and Te) Using ATK-DFT," *Metallurgical and Materials Engineering*, **26**(3), 253-278 (2020). <https://doi.org/10.30544/475>
- [56] M. Ahmad, G. Rehman, L. Ali, M. Shafiq, R. Iqbal, R. Ahmad, T. Khan, S. Jalali-Asadabadi, *et al.* "Structural, electronic and optical properties of CsPbX_3 (X= Cl, Br, I) for energy storage and hybrid solar cell applications," *Journal of Alloys and Compounds*, **705**, 828-839 (2017). <https://doi.org/10.1016/j.jallcom.2017.02.147>
- [57] A.V. Kuklin, and H. Ågren, "Quasiparticle electronic structure and optical spectra of single-layer and bilayer PdSe_2 : Proximity and defect-induced band gap renormalization," *Physical Review B*, **99**(24), 245114 (2019). <https://doi.org/10.1103/physrevb.99.245114>
- [58] S. Chahar, K.K. Mishra, and R. Sharma, "Investigation of Structural, Electronic, and Optical Characteristics of a Novel Perovskite Halide, Mg_3AsCl_3 , for Electronic Applications," *Physica status solidi (b)*, 2400171. <https://doi.org/10.1002/pssb.202400171>
- [59] P. Barman, Md.F. Rahman, Md.R. Islam, M. Hasan, M. Chowdhury, M.K. Hossain, J.K. Modak, *et al.* "Lead-free novel perovskite Ba_3AsI_3 : First-principles insights into its electrical, optical, and mechanical properties," *Heliyon*, **9**(11), (2023). <https://doi.org/10.1016/j.heliyon.2023.e21675>
- [60] Md.S. Alam, Md. Saiduzzaman, A. Biswas, T. Ahmed, A. Sultana, and K.M. Hossain, "Tuning band gap and enhancing optical functions of AGeF_3 (A= K, Rb) under pressure for improved optoelectronic applications," *Scientific Reports*, **12**(1), 8663 (2022). <https://doi.org/10.1038/s41598-022-12713-4>
- [61] M.H.K. Rubel, M.A. Hossain, M.K. Hossain, K.M. Hossain, A.A. Khatun, M.M. Rahaman, Md.F. Rahman, *et al.* "First-principles calculations to investigate structural, elastic, electronic, thermodynamic, and thermoelectric properties of $\text{CaPd}_3\text{B}_4\text{O}_{12}$ (B=Ti,V) perovskites," *Results in Physics*, **42**, 105977 (2022). <https://doi.org/10.1016/j.rinp.2022.105977>
- [62] A. Ghosh, Md.F. Rahman, Md.R. Islam, Md.S. Islam, M.K. Hossain, S. Bhattarai, R. Pandey, *et al.* "Structural, electronic and optical characteristics of inorganic cubic perovskite Sr_3AsI_3 ," *Optics Continuum*, **2**(10), 2144-2153 (2023). <https://doi.org/10.1364/optcon.495816>
- [63] Md.Z. Rahman, S.S. Hasan, Md.Z. Hasan, Md. Rasheduzzaman, Md.A. Rahman, Md.M. Ali, A. Hossain, *et al.* "Insight into the Physical Properties of the Chalcogenide XZrS_3 (X= Ca, Ba) Perovskites: A First-Principles Computation," *Journal of Electronic Materials*, 1-17 (2024). <https://doi.org/10.1007/s11664-024-11120-x>
- [64] A. Ghosh, Md.F. Rahman, Md.R. Islam, Md.S. Islam, M. Amami, M.K. Hossain, and A.B.Md. Ismail, "Inorganic novel cubic halide perovskite Sr_3AsI_3 : Strain-activated electronic and optical properties," *Heliyon*, **9**(8), no. 8 (2023). <https://doi.org/10.1016/j.heliyon.2023.e19271>
- [65] D.O. Obada, S.B. Akinpelu, S.A. Abolade, E. Okafor, A.M. Ukpung, Syam Kumar R, and A. Akande, "Lead-free double perovskites: a review of the structural, optoelectronic, mechanical, and thermoelectric properties derived from first-principles calculations, and materials design applicable for pedagogical purposes," *Crystals*, **14**(1), 86 (2024). <https://doi.org/10.3390/cryst14010086>

АНАЛІЗ СТРУКТУРНИХ, ЕЛЕКТРОННИХ ТА ОПТИЧНИХ ВЛАСТИВОСТЕЙ ПЕРОВСКІТУ Ca_3PbCl_3 ДЛЯ ЗАСТОСУВАННЯ В ЗЕЛЕНІЙ ЕНЕРГЕТИЦІ ТА ОПТОЕЛЕКТРОНІЦІ

Чакшу Малан¹, Крішна Кумар Мішра¹, Раджніш Шарма²

¹Інститут інженерії та технологій Університету Чіткара, Університет Чіткара, Раджпура, Пенджаб-140401, Індія

²Школа інженерії та технологій Університету Чіткара, Солан, Хімачал-Прадеш-174103, Індія

Метою цього дослідження є детальне вивчення способів покращення ефективності перовскіту Ca_3PbCl_3 в оптоелектронній галузі та галузі сонячних елементів. Речовина, відома як Ca_3PbCl_3 , класифікується в тій самій категорії, що й перовскіти, що складаються з неорганічних галогенідів металів. У рамках цього дослідження для вивчення оптичних, електричних та структурних характеристик було використано теорію функціоналу густини (DFT), яка є базовими принципами. Узагальнене градієнтне наближення (GGA), функціонали Пердю Берка-Ернцєргофа та калькулятор лінійної комбінації атомних орбіталей – це інструменти, які використовуються для розуміння характеристик перовскіту Ca_3PbCl_3 . Ключовим моментом є ширина забороненої зони матеріалу, яка, за вимірюваннями, становить 20,35 eV у точці Г. Також було виявлено, що діелектрична функція та спектри поглинання змінюються залежно від енергії фотона. Повідомлялося, що значення коефіцієнта екстинкції становить $3,6963 \times 10^4$, а значення показника відбиття – 1,4410. Тому вивчення оптичних властивостей Ca_3PbCl_3 має вирішальне значення для розгляду цього матеріалу для майбутнього використання у фотоелектричних та оптоелектронних пристроях.

Ключові слова: структурні властивості; оптичні властивості; електричні властивості; розділення шарів